A Novel Direct-Detection Doppler Wind Lidar Based on a Fringe-Imaging Michelson Interferometer as Spectral Analyzer

***P. Vrancken*[1], *J. Herbst*[1,2]**
(1) Institute of Atmospheric Physics, German Aerospace Center (DLR), 82234 Weßling, Germany
(2) now with ARRK Engineering, 85049 Ingolstadt, Germany
Email: patrick.vrancken@dlr.de

We report on the development of a novel direct-detection Doppler wind lidar (DD-DWL) featuring – in our view – several advantages over most DD techniques employed today. The main novel technological aspects are the use of a field-widened monolithic Michelson interferometer, a linear detector array for 1D-compressed fringe imaging and optical fibers for efficient beam scrambling and forming (Herbst & Vrancken, 2016; Vrancken & Herbst, 2019).

We are investigating the use of DWLs as sensor within feedforward gust load alleviation control loops on fast-flying fixed-wing aircraft. From these rather unusual requirements stems the special design presented here. However, we are convinced the general layout would also benefit other DD-DWL applications such as ground-based or airborne atmospheric research up to spaceborne global wind observation as in envisioned Aeolus follow-on missions. The aeronautics forward-pointing turbulence mitigation scheme (Vrancken, 2016) imposes the following requirements on the lidar system: sub-m/s precision, high data repetition rate (few to several tens of Hz), high spatial resolution (20 to 50m), close measurement ranges (50 to 300m) as well as sensitivity to both mixed molecular and aerosol and pure molecular backscatter without knowledge on the ratio thereof (i.e., backscatter ratio).

The current development (termed 'AEROLI') so far exclusively focuses on the DD-DWL receiver alone since we may use the well proven airborne WALES/DELICAT (Vrancken et al., 2016; Wirth et al., 2009) laser transmitter, a tripled Nd:YAG MOPA delivering 75 mJ, 8 ns, 150 MHz, 355 nm UV pulses locked onto an iodine-line. As optical front-end for collection of the backscattered radiation we employ an equally flight-proven (Vrancken et al., 2016) system with a monostatic, co-axial, 6" *f*/8 Newton telescope, collimator, 0.5 nm narrow interference filter, and large-core multi-mode fiber injection.

The approach of the novel direct detection receiver is based on the illumination of a field-widened Michelson interferometer which allows for both large acceptance angles (necessary since working in the near field) and a certain insensitivity to angular transmit beam fluctuations (due to vibrations, e.g.). A slightly skewed mirror within the Michelson yields a linear fringe for Doppler spectral analysis by fringe-imaging which makes the measurement independent of the knowledge on the current backscatter ratio R_b.

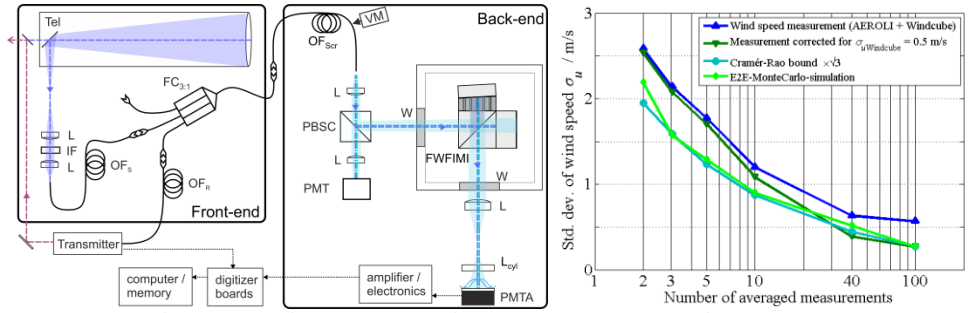

Figure 1: Simplified synopsis of DWL receiver (left panel). Right: Expected performance based on theoretical Cramér-Rao bound (cyan) for a Michelson spectral analyzer and end-to-end simulations (light green). The graph also shows (blue, green) determined measurement performance, see Fig. 2.

The linear fringe enables a 1-D compression along one axis (by a cylindrical lens) and thus imaging onto a fast linear detector (PMT array). These PMTs and fast multichannel ADCs yield highly range resolved signals, both backscattered atmospheric ones as well as reference signals provided by the laser source. The general physical layout of the monolithic Michelson interferometer with an air arm and a glass arm (optically contacted parts) is highly vibration resilient and features a temperature compensation. As mentioned above, the backscattered radiation from the telescope is injected into a series of large-core multimode optical fibers of various geometries (circular, hexagonal and quadratic) for scrambling of the geometric (angular-spectral) information and (quadratic) for an efficient illumination of the interferometer.

For final wind speed retrieval, the fringe amplitude signals (approximate cosine form) are corrected by an illumination function. This function is determined by a laser frequency sweep over the Michelson free

spectral range (*FSR*). After range and time averaging, the atmospheric (wind) and reference (laser) fringes are approximated by a four-parameter fit function with the phase comparison directly yielding the wind speed, a shift of 5.6 MHz (≈ 1/1900 of the *FSR* of 10.7 GHz) translating to 1 m/s.

Along with the hardware development, a thorough end-to-end (E2E) Monte-Carlo simulation environment has been set up, including several relevant noise sources such as photon and detector noise, atmospheric and fiber speckle noise. The estimated performance with an arbitrary number of photons is given (over some pulses averaging) in Fig. 1 (right) along with the theoretically achievable limit, given by the Cramér-Rao bound (CRB) of such a spectral analyzing estimator. The roughly $\sqrt{3}$ discrepancy between the CRB and E2E simulations (and also measurements) represents such noise contributions (that are not covered by the pure photon-noise relating CRB).

A first compact DD-DWL of the described subsystems has been ground-tested in 2018 (and is currently under further development and test with several hardware improvements) against a commercial coherent DWL, a Leosphere Windcube© 200S. So far, we operated the lidar in a sub-optimum, non-photon-number optimized way, with multiple optical inefficiencies and residual misalignments, and focused on the Doppler spectral analysis.

Ground-based horizontal and vertical wind measurements demonstrate its ability of measuring close-range wind speeds with a precision of 0.5 m/s, independent of the actual wind speed value. For instance, as displayed in Fig. 2, arbitrary ground winds are averaged over 40 laser pulses (i.e. at 2.5 Hz) and aggregated to 30 m range gates (6 × 30 MHz samples) for AEROLI, and for the Windcube© at 2 Hz and 25 m range gate. This led to a combined distribution over the whole 15 min dataset of 0.7 m/s. Attributing comparable distributions for both DWL systems (also conforming to Leosphere data), this yields 0.5 m/s precision for this 2.5 Hz averaging, and accordingly higher for shorter averaging as indicated in Fig. 1.

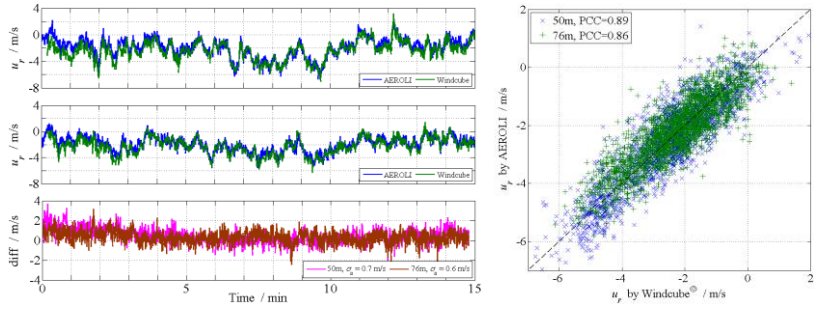

Figure 2: Time series of wind measurements at two closes ranges (50 and 76 m) of the AEROLI DD-DWL and Leosphere Windcube© 200 and respective differences (left, lower panel) after bias correction. The right diagram shows the respective distribution and the Pearson correlation coefficients.

Despite these first positive outcomes, we still have numerous – but now known – challenges to face, such as important range and time-dependent bias to start with. A key point of ongoing investigations is the above mentioned illumination function. Apart from this, we strive also to advance the system towards satisfying optical efficiencies. These improvements in performance shall be consolidated by a series of ground-based local and high-altitude tests.

References

Herbst, J., & Vrancken, P. Design of a monolithic Michelson interferometer for fringe imaging in a near-field, UV, direct-detection Doppler wind lidar. *Applied Optics*, *55*(25), 6910, 2016. https://doi.org/10.1364/AO.55.006910

Vrancken, P. Airborne remote detection of turbulence with forward-pointing LIDAR. In R. Sharman & T. Lane (Eds.), *Aviation Turbulence*. Springer International Publishing, 2016. https://doi.org/10.1007/978-3-319-23630-8

Vrancken, P., & Herbst, J. Development and Test of a Fringe-Imaging Direct-Detection Doppler Wind Lidar for Aeronautics. *EPJ Web of Conferences*. 29th International Laser Radar Conference, Hefei, People's Republic of China, 2019.

Vrancken, P., Wirth, M., Ehret, G., Barny, H., Rondeau, P., & Veerman, H. Airborne forward-pointing UV Rayleigh lidar for remote clear air turbulence detection: System design and performance. *Applied Optics*, *55*(32), 9314, 2016. https://doi.org/10.1364/AO.55.009314

Wirth, M., Fix, A., Mahnke, P., Schwarzer, H., Schrandt, F., & Ehret, G. The airborne multi-wavelength water vapor differential absorption lidar WALES: System design and performance. *Applied Physics B*, *96*(1), 201–213, 2009. https://doi.org/10.1007/s00340-009-3365-7